RAPID COMMUNICATIONS

PHYSICAL REVIEW A VOLUME 39, NUMBER 5 MARCH 1, 1989

Nonlinear competition between waves on convective rolls

Vincent Croquette and Hugh Williams
AT&T Bell Laboratories, Murray Hill, New Jersey 07974
(Received 15 July 1988)

We report experimental observations of confined and temporally modulated states produced by the oscillatory instability of straight convective rolls. For this system we have measured all the critical parameters characterizing the instability. We are thus able to confirm the interpretation of such phenomena proposed by Cross [Phys. Rev. A **38**, 3593 (1988)] based on the combination of propagative effects and finite geometry.

The stability of systems that bifurcate to a wave state involving both a temporal frequency and a spatial wave number is the subject of many current studies. In particular, observations of traveling waves in binary mixtures,[1,2] in Taylor-Couette experiments,[3] and in the oscillatory instability of convective rolls[4] have revealed unusual localized as well as time-modulated states. Conflicting theories have been proposed to explain these phenomena.[5-7] We have studied the oscillatory instability of Rayleigh-Bénard convective rolls at low Prandtl number and have observed similar complex spatiotemporal behavior. By determining the amplitude-equation parameters for this system, we have confirmed the scheme proposed by Cross based on the propagative nature of the instability and the interplay of the right and left waves coupled through the sidewall reflection.

When a temperature difference ΔT is applied vertically across a horizontal fluid layer of thickness d, the first bifurcation to the convective state takes place when the Rayleigh number R ($\propto \Delta T$) exceeds a critical value R_c. In fluids with a low Prandtl number $\mathcal{N}_{\rm Pr}=\nu/\kappa$ (where ν is the kinematic viscosity and κ the thermal diffusivity), a secondary bifurcation to a state in which transverse waves propagate along the rolls takes place at a higher Rayleigh number R_1 which depends on $\mathcal{N}_{\rm Pr}$ and on the roll wave number k_x. This is the oscillatory instability of Busse.[8]

The convection cell consists of a plastic frame of thickness $d=1$ mm and horizontal size $24d\times 31.7d$. This frame is sandwiched between a thick, water-cooled sapphire window and a copper mirror. This cell is placed in a pressurized container, and observation is achieved by shadowgraphy. The fluid is argon at 60 atm, leading to $\tau_v=d^2/\kappa=2.72$ s for the vertical diffusion time, $\mathcal{N}_{\rm Pr}=\nu/\kappa=0.7$, and $\Delta T=3.474$ K at R_c.

The characterization of the oscillatory instability requires straight rolls, which are not commonly observed experimentally.[9] To prepare a straight-roll pattern, we have placed small heating wires along the two short sidewalls of the rectangular cell. This forcing generates the seed from which the roll pattern ultimately develops. For this system, the oscillatory instability will appear if the wave number k_x of the rolls equals approximately $\frac{2}{3}$ of the critical wave number k_{xc}, and if R is 3 to 4 times R_c.[10] Otherwise, different instabilities occur. Starting at R_c with 30 straight rolls, we must remove 5 roll pairs while increasing R to obtain the final 20 rolls. We do this by applying a short and strong alternating flow through the filling hole located in the center of the long side of the container, using a small loudspeaker. This induces a dislocation which climbs through the pattern. By using this technique we have measured the stability diagram of these convective rolls and their defects, as we described in Ref. 11.

Just above $R_1=3.929R_c$, the rolls start to oscillate about their mean positions. Two waves traveling along the y direction can be seen, each heading to the nearest long sidewall. As shown in Fig. 1, the oscillations are in phase from roll to roll, their magnitudes decaying near the short sidewalls. Using a video camera, we measure, in real time, the displacement $\delta x(y,t)$ of one roll (with its axis along y) as a function of the position along the roll y and of time t. We scale the measure of δx by d. In Fig. 2(a) we show the time and space evolution of $\delta x(y,t)$ for $R=4.222R_c$. In two-dimensional (2D) space (y,t), the right and left waves correspond to two distinct Fourier modes centered on (k_{y0},ω_0) and $(-k_{y0},\omega_0)$ which may thus be separated to obtain the complex amplitude A_r (A_l) of the right (left) wave with the fast spatial and temporal scales removed.[12]

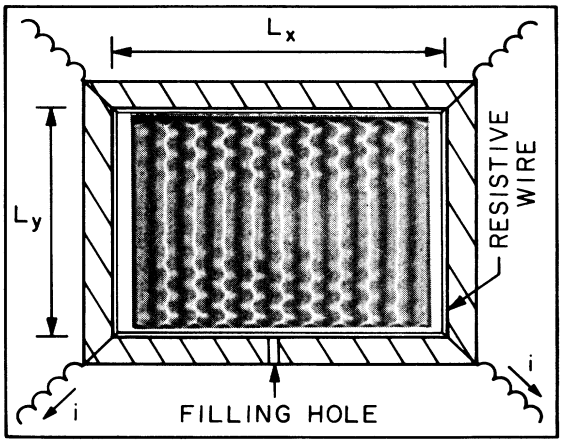

FIG. 1. Picture of the oscillatory instability occurring on a pattern of 20 straight rolls at $R=4.3R_c$ with $k_x=1.98$. The picture is enclosed by a sketch of the container showing the resistive wires along the short sidewalls and the location of the filling hole connected to the loudspeaker. The length of the cell L_x has been expanded to make the wires visible.

The oscillatory instability appears via a forward Hopf bifurcation. In a range $R_1 < R < R_3 = 4.283 R_c$, the time evolution is monoperiodic with $f \approx 1.2$ Hz. As shown in Fig. 2, the amplitudes of the waves grow exponentially as they travel along the roll. For $R_1 < R < R_2$, the maximum amplitudes of both waves are the same, as shown in Fig. 3. At $R_2 = 4.12$, a new forward bifurcation leads to a symmetry breaking, and one wave progressively dominates the other, as in Fig. 2(c). Above R_3, a slow modulation of the fundamental frequency appears. Between R_3 and $R_4 = 4.352 R_c$, the modulation is periodic and represents the beating of the dominant wave and the small one at a frequency $\omega/51$. Over a small range of temperature, this modulation leads to a subharmonic bifurcation and then to chaos. When R is increased further, the dominant wave alternates from right to left, but simultaneously the phase coherence from roll to roll is lost, and the phenomenon becomes two dimensional and beyond the scope of this study.

The waves may be described by Landau-Ginsburg (LG) coupled amplitude equations.[12] In this particular case, Fauve, Bolton, and Brachet[13] have derived them as

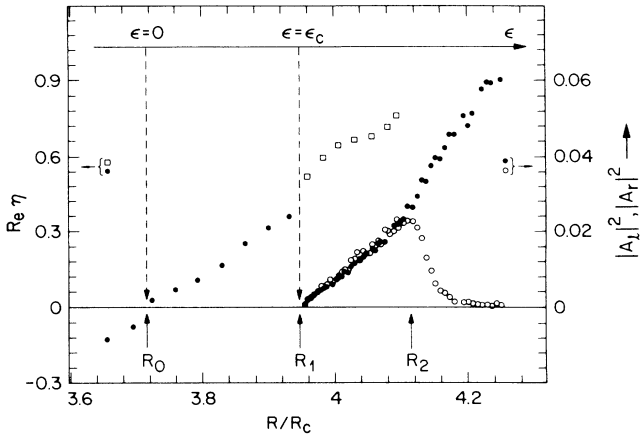

FIG. 3. Bifurcation diagram. The maximum value of $|A_r|$ and $|A_l|$ are scaled with d and plotted vs R. The points on the left correspond to the growth rate η (measured by using the loudspeaker for $\epsilon < \epsilon_c$ and directly from the pattern otherwise). These measurements lead to the determination that $\epsilon = 0$ at $R = R_0 = 3.727 R_c$.

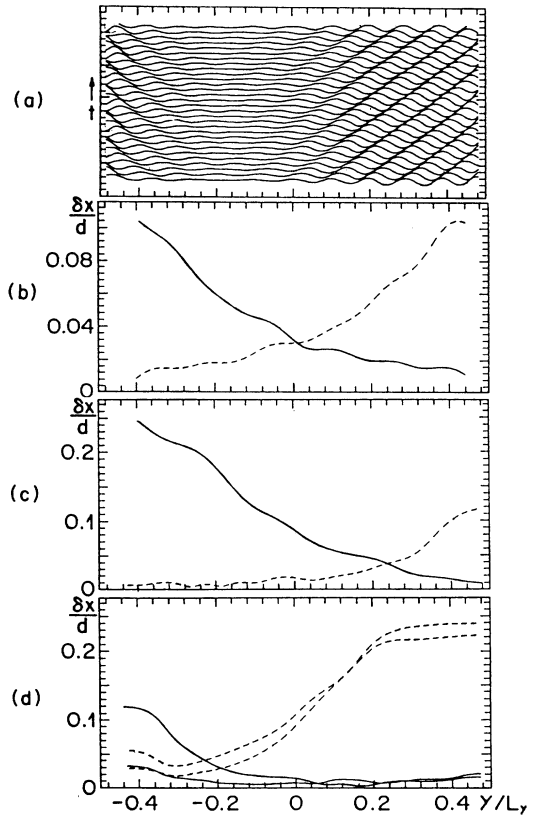

FIG. 2. (a) Plot of the roll displacement $\delta x(y,t)$ at $R = 4.222 R_c$, corresponding to the case where one wave dominates. (b) Amplitude of the right and left wave along the roll at $R = 4.036 R_c$, when both are symmetrical. (c) $R = 4.222 R_c$; one wave dominates. (d) $R = 4.349 R_c$; the two waves are beating. The two lines correspond to two opposite phases of the modulation period.

follows:

$$\tau_0(\partial_t + s\partial_y)A_r = \epsilon z_0 A_r + \xi_0^2 z_1 \partial_y^2 A_r - g z_2(|A_r|^2 + 2|A_l|^2)A_r , \quad (1a)$$

$$\tau_0(\partial_t - s\partial_y)A_l = \epsilon z_0 A_l + \xi_0^2 z_1 \partial_y^2 A_l - g z_2(|A_l|^2 + 2|A_r|^2)A_l , \quad (1b)$$

with $z_i = 1 + i c_i$, c_i being real; A_r (A_l) is the amplitude of the right (left) wave, with the rapid time frequency ω and spatial frequency k_y ($-k_y$) removed. Finally, $\epsilon \propto R$. Equations (1a) and (1b) extend the one describing a stationary pattern:[14] τ_0 is the characteristic time scale, ξ_0 the correlation length, ϵ the control parameter, and g measures the nonlinear saturation. The waves are, moreover, characterized by their group velocity $s = d\omega/dk_y$ and lead to complex parameters. The c_i express the evolution of the wave frequency ω with each parameter: c_0 with ϵ, c_1 with $Q^2 (Q = k_y - k_{y0})$, and c_2 with the amplitude of oscillation.

In contrast to the case of a stationary pattern, the parameters of the LG equations [Eqs. (1a) and 1(b)] may not all be absorbed by a proper rescaling of variables, so that different physical behavior may be expected depending upon these parameters. To determine them, we have used the loudspeaker connected to the filling hole to generate a small localized and periodic perturbation which is ideal for inducing oscillations on the roll. When R is just smaller than R_1, and $\omega \approx \omega_0$, this perturbation leads to a traveling wave with a wave number k_y and an amplitude which grows exponentially along the roll, its growth-rate being η_y. Keeping R constant and scanning ω, we determine k_y and η_y. The dispersion relation is given in Fig. 4 and may be written as $\mathrm{Im}\eta = \omega = \omega_0 + sQ + c_1(\xi_0^2/\tau_0)Q^2 - (c_0/\tau_0)\epsilon$. From η_y and s, we obtain the temporal growth rate: $\mathrm{Re}\eta = (\epsilon/\tau_0) - (\xi_0^2/\tau_0)Q^2$. Both agree with predictions.[10] This gives all the critical parameters in-

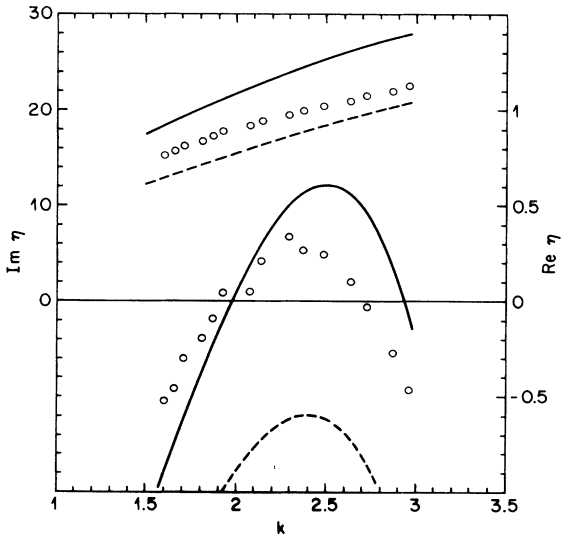

FIG. 4. Dispersion relation of the oscillatory instability determined just below ϵ_c ($R=3.92R_c$). The open circles correspond to this experiment; $\mathrm{Im}\eta=\omega$ and η have been normalized using τ_v. Solid (dashed) line corresponds to the prediction of Clever and Busse (Ref. 10) with $\mathcal{N}_{\mathrm{Pr}}=0.71$, $k_y=2.0$, and $R=4.098R_c$ ($R=2.927R_c$).

volved in the linear parts of Eqs. (1a) and (1b): $dk_{y0}=2.3\pm0.1$, $\tau_v\omega_0=19.8\pm1$, $\tau_v d^{-1}s=5.02\pm0.5$, $d^{-1}\xi_0=0.52\pm0.15$, $\tau_v^{-1}\tau_0=0.163\pm0.05$, $c_0=1.57\pm0.3$, and $c_1=-0.826\pm0.3$. Finally, by setting $\omega=\omega_0$ and varying R, we determine the R_0 value corresponding to $\epsilon=0$. For $R_0<R<R_1$, the sidewall-reflection losses prevent the instability from developing. The value of $\epsilon_c=0.058$ corresponding to $R=R_1$ is related to the sidewall reflection r by $e^{\epsilon_c L_y/\tau_0 s}=1/r$, leading to $r=0.183$.

The nonlinear parameter g should be given by the linear behavior of $|A_{r,l}|^2$ with ϵ. Since this asymptotic regime is not reached in Fig. 3, we give a lower limit of $g\geq 2.3$. We have estimated c_2 using the state shown in Fig. 2(c). The local wave number k_y increases as the amplitude of the strongest wave reaches its maximum, leading to $c_2=-1.15$.

The waves are characterized by two velocities: the group velocity s, and a front velocity $v_f=n\epsilon^{1/2}\xi_0/\tau_0$. If we are in a frame moving at the velocity s, v_f characterizes the invasion speed of a saturated oscillating state into the unstable rest state; n is a numerical factor depending on Eqs. (1a) and (1b), $n=2$ when $c_1=c_2=2$. According to the ratio of the two velocities, a pulse launched along the roll will either spread everywhere, this is the *absolute* instability, or will be swept away with the group velocity, this is the *convective* instability. The transition between the two regimes occurs when $\bar{s}=s\tau_0/\epsilon^{1/2}\xi_0$ exceeds 2. Since v_f varies as $\sqrt{\epsilon}$, $\bar{s}$ will diverge as $\epsilon\rightarrow 0$. However, the sidewall-reflection losses prevent the occurrence of the instability when $0<\epsilon<\epsilon_c$. This limits the value reached by $\bar{s}$. For our experiment, we find that $\bar{s}=\bar{s}_c=6.5\pm2$ at ϵ_c, and its value remains bigger than 2 when we reach the chaotic state. Although the concepts of *absolute* and *convective* instabilities were defined for an infinite system,[15] Cross has shown that in a finite container they will lead to very different patterns.[16] We confirm that in the *convective* case the waves are localized since they exhibit an exponential profile reaching a significant amplitude only near the sidewall.

Our observations bear many similarities with those made in binary mixtures[1,2] as well as in convection in mercury.[4] However, those examples involve a subcritical bifurcation, which adds extra possibilities to explain localized states. Nonlinear waves are particularly interesting since the equations governing them [Eqs. (1a) and (1b)] lead to intrinsic time dependence as soon as c_1 and $c_2\neq0$. In this situation, the Benjamin-Feir instability[17] may be expected and was invoked to explain time dependence in previous experiments. In our case, we believe that the longitudinal Benjamin-Feir instability *is not* relevant since the product c_1c_2 is positive leading to the stability versus longitudinal phase disturbances.[17] To confirm this stability, we have checked that the wave number k_y always lies in the stable band when R is increased. Using a model with $c_1=c_2=0$, Cross has shown that the nonlinear competition between modes may also explain wave beating. Profiles of the waves of Fig. 3(d) are very similar to those calculated by Cross and occur in the same range of $\bar{s}$. In addition, the slow amplitude modulation frequency is in the range of $4L_y/s$ in the numerical simulation, and $3.37L_y/s$ in the experiment. In the regime where waves are in phase from roll to roll, our experiment fully confirms Cross's simulations. Although we are not truly in the regime $c_1=c_2=0$, we confirm these ideas. On the other hand, the negative value of c_2 may lead to transverse phase instability, which may be related to bidimensional time dependence that we have observed and should lead to further studies.

We have characterized the oscillatory instability occurring on straight convective rolls in gases. We confirm the idea proposed by Cross that waves in a finite container having a *convective* nature lead to confined states and time dependence. The understanding of this mechanism, as well as the complete determination of the critical parameters involved in the oscillatory instability, are essential steps to study the phase dynamics of waves and their related instability.

We wish to acknowledge P. Kolodner, C. M. Surko, M. C. Cross, P. C. Hohenberg, D. Bensimon, B. Shraiman, and W. Van Saarloos for enlightening discussions. V.C. thanks Centre National de la Recherche Scientifique for financial support.

[1]E. Moses, J. Fineberg, and V. Steinberg, Phys. Rev. A **35**, 2757 (1987); R. Heinrichs, G. Ahlers, and D. S. Cannell, Phys. Rev. A **35**, 2761 (1987).

[2]P. R. Kolodner and C. M. Surko, Phys. Rev. Lett. **61**, 842 (1988); J. Fineberg, E. Moses, and V. Steinberg, Phys. Rev. Lett. **61**, 842 (1988).

[3]C. D. Andereck, S. S. Liu, and H. L. Swinney, J. Fluid Mech. **164**, 155 (1986).

[4]A. Chiffaudel, B. Perrin, and S. Fauve, preceding paper, Phys. Rev. A **39**, 2761 (1989).

[5]P. Coullet, S. Fauve, and E. Tirapegui, J. Phys. (Paris) Lett. **46**, 787 (1985).

[6]H. R. Brand, P. S. Lomdahl, and A. C. Newell, Physica D **23**, 345 (1986).

[7]M. C. Cross, Phys. Rev. Lett. **57**, 2935 (1986).

[8]F. H. Busse, J. Fluid Mech. **52**, 97 (1972).

[9]A. Pocheau, V. Croquette, and P. Le Gal, Phys. Rev. Lett. **55**, 1097 (1985).

[10]R. M. Clever and F. H. Busse, J. Fluid Mech. **65**, 625 (1974).

[11]V. Croquette and H. Williams, in *Proceedings of Advances in Fluid Turbulence, Los Alamos, 1988* [Physica D (to be published)]; see also V. Croquette, Contemp. Phys. (to be published).

[12]A. C. Newell and J. A. Whitehead, J. Fluid Mech. **38**, 279 (1969).

[13]S. Fauve, E. W. Bolton, and M. E. Brachet, Physica D **29**, 202 (1987).

[14]J. E. Wesfreid, Y. Pomeau, M. Dubois, C. Normand, and P. Bergé, J. Phys. (Paris) **39**, 725 (1978).

[15]E. M. Lifshitz and L. P. Pitaevskii, *Physical Kinetics* (Pergamon, New York, 1981), p. 268; R. J. Diessler, Physica D **25**, 233 (1987).

[16]M. C. Cross, Phys. Rev. A **38**, 3593 (1988).

[17]T. B. Benjamin and J. E. Feir, J. Fluid Mech. **27**, 417 (1966); J. T. Stuart and R. C. DiPrima, Proc. R. Soc. London, Ser. A **362**, 27 (1978).

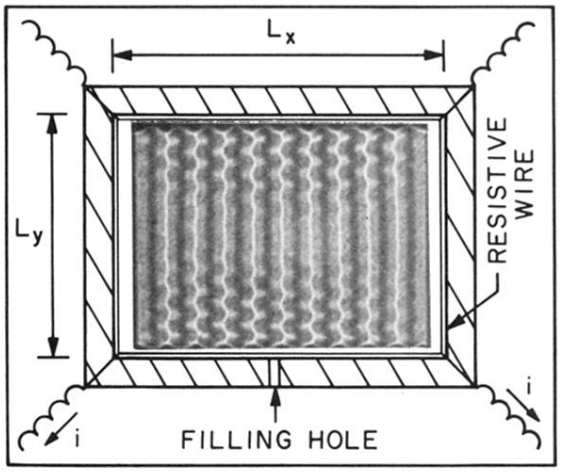

FIG. 1. Picture of the oscillatory instability occurring on a pattern of 20 straight rolls at $R=4.3R_c$ with $k_x=1.98$. The picture is enclosed by a sketch of the container showing the resistive wires along the short sidewalls and the location of the filling hole connected to the loudspeaker. The length of the cell L_x has been expanded to make the wires visible.